Computational Engineering and Technology Innovations

www.ceti.reapress.com

Comput. Eng. Technol. Innov. Vol. 2, No. 3 (2025) 11–28.

Paper Type: Original Article

Enhanced Brain Tumour Detection Using Adaptive Preprocessing and Hybrid Deep Learning Techniques

Javad Pourqasem[1], Zeynab Parandavar[2,*]

[1] Department of Computer Engineering, Ayandegan Institute of Higher Education, Tonekabon, Iran; z.parand.1997@gmail.com.
[2] Department of Computer Engineering and Mathematics, Morvarid Intelligent Industrial Systems Research Group, Iran; z.parand.1997@gmail.com.

Citation:

Received: 17 October 2024 *Revised: 29 December 2024* *Accepted: 04 March 2025*	Pourqasem, J., & Parandavar, Z. (2025). Enhanced brain tumour detection using adaptive preprocessing and hybrid deep learning techniques. *Computational Engineering and Technology Innovations*, *2*(3), 11-28.

Abstract

Magnetic Resonance Imaging (MRI) is a crucial diagnostic tool for neurological and brain cancers, which are major global health issues. However, hand-analysed MRI scans are inconsistent and time-consuming. This paper describes a sophisticated strategy for employing Dynamic Contrast-Enhanced Magnetic Resonance Imaging (DCE-MRI) to detect brain cancers. By combining hybrid Deep Learning (DL) algorithms with superior preprocessing, the framework improves performance. Initially, Adaptive Multi-scale Gaussian Filtering (AMGF) is applied to minimize noise and improve image quality. Following the identification of the most relevant features using Recursive Feature Elimination with Cross-Validation (RFECV), Lévy Flight Particle Swarm Optimization (LFPSO) is used to optimize feature extraction. To perform classification, a hybrid DL model combines Convolutional Neural Networks (CNNs) with Long Short-Term Memory (LSTM) networks, identifying both temporal and spatial patterns accurately. This technique provides significant increases in detection accuracy and processing performance. indicating its potential for clinical use and better patient outcomes. The results shown that the proposed method has the best results around the comparison methods.

Keywords: Magnetic resonance imaging, Brain tumor detection, Adaptive preprocessing, Hybrid deep learning, Dynamic contrast-enhanced magnetic resonance imaging, Convolutional neural network, Long short-term memory.

1 | Introduction

Accurate brain tumour classification is crucial for early identification and therapy. Magnetic Resonance Imaging (MRI) generates the high-contrast images necessary for non-invasive tumor identification. This study examines two cutting-edge methods: EfficientNets-based Transfer Learning (TL) diagnoses cancers as glioma, meningioma, or pituitary tumors with an accuracy of 99.06% and F1-scores of 98.79%. Furthermore, for detections and classifications, the Exponential Deer Hunting Optimization (ExpDHO)-based Deep

Corresponding Author: z.parand.1997@gmail.com
https://doi.org/10.48314/ceti.vi.77
Licensee System Analytics. This article is an open-access article distributed under the terms and conditions of the Creative Commons Attribution (CC BY) license (http://creativecommons.org/licenses/by/4.0).

Convolutional Neural Network (DCNN) with Exponential Deer Hunting Optimization-based Shepard Convolutional Neural Network (ExpDHO-based ShCNN) are employed. This method includes noise reduction, image segmentation, and augmentation, achieving high performance with sensitivity of 0.939, and specificity of 0.919 [1], [2]. Image segmentations are vital yet challenging for diagnosing brain tumors, which affect essential Central Nervous System (CNS) functions. MRI is a standard tool for detecting these tumors, but classification can be difficult. Thes study introduces two advanced methods where Adaptive Flying Squirrel Algorithm segmented tumors while Adaptive Fuzzy Deep Neural Networks (DNNs) with Frog Leap Optimizations classified MRI image. The first technique, which is implemented in MATLAB, yields 99.8% specificity, 99.9% sensitivity, and 99.6% accuracy. Furthermore, DeepTumorNet, a hybrid GoogLeNet-based Deep Learning (DL) model, provides exceptional classification for glioma, meningioma, and pituitary tumors, with 99.67% accuracy and 100% recall [3], [4]. Brain tumor classifications are crucial in medical imaging for effective diagnosis and treatments. An Optimized Hybrid Deep Neural Network (OHDNN) that improves brain tumour identification through two primary stages pre-processing and classification is presented in this research. Enhancement and noise reduction are the first steps used to improve MRI images. Adaptive Rider Optimizations (AROs) enhance OHDNN performances as Long Short-Term Memories (LSTMs) classify while features are extracted using Convolution Neural Networks (CNNs). The approach achieves up to 97.5% accuracy. Additionally, the paper addresses MRI image segmentation, highlighting preprocessing methods, CNN-based segmentation, and the impact of strength normalization and data augmentation on accuracy [5], [6].

A novel approach that uses sophisticated segmentation algorithms on MRI images to identify brain tumors. For improved tumor detection, the method makes use of CNNs and inception modules, leveraging current developments in DL. Despite differences in data, automated segmentation increases speed and uniformity. Significant improvements in dice score, sensitivity, and specificity are demonstrated by new DNN designs like Multi-Image type UNet (MI-UNet) and depth-wise separable MI-Unets where the latter performs better. A CNN-LSTM model enhances the suggested hybrid DL strategy, which combines Stationary Wavelet Packet Transform (SWPT) for feature extractions and Adaptive Kernel Fuzzy C-Means (AKFCM) for segmentations. Evaluated in MATLAB, the method demonstrates high accuracy and precision [7], [8]. The Accurate brain tumor classification is vital for early diagnosis and treatment. This study proposes an advanced AI-based framework combining Vision Transformer (ViT) and DNNs for enhanced classification. The framework includes preprocessing, data normalization, and feature extraction using Haralick features and local binary patterns. Optimized CNN capture local details, while ViT manages long-range dependencies. The features are weighed, fused, and classified using Machine Learning (ML) models. Evaluated on multiple MRI datasets, this ensemble approach shows improved performance. Additionally, the paper's usages of DCNNs with Harris Hawks Optimizations (HHO) and Grey Wolf Optimizations (GWO), achieved 97% accuracy with enhanced speed and reduced memory usages [9], [10]. These research focuses on improving brain tumor detections through an integrated approach that incorporated pre-processes using Dynamic Contrast-Enhanced Magnetic Resonance Imaging (DCE-MRI) for feature selections, extractions, and classifications. Adaptive Multi-scale Gaussian Filtering (AMGF) improved image qualities by reducing noises and boosting contrasts, two elements required for successful feature extractions. Recursive Feature Elimination with Cross-Validation (RFECV) chose the best features, and Lévy Flight Particle Swarm Optimization (LFPSO) effectively extracts key features from MRI images. Classifications were performed using hybrid DL models that combined CNNs and LSTMs to capture both temporal and spatial data. The new method when compared to existing methodologies, revealed significant improvements in tumour identifications and obtained better values for accuracy, sensitivity with processing efficiency [10].

The remainder of this study activity is organized as follows. Section 2 provides a brief summary of some recent research in the areas of preprocessing, feature extraction, feature selection, and illness classification. Section 3 describes the suggested approach for the CNN-LSTM system. The experimental performance analysis results are given in Section 4, and Section 5 concludes with summarizing the results.

2 | Related Work

A thorough overview and critical study on identifications and classifications of brain tumours using MRI images and DL algorithms can be found in, by Nazir et al. [9]. The study starts with an overview of earlier research in this field, and is intended at DL specialists who are interested in using their expertise to examine brain tumours. Next, it provides a thorough analysis of DL techniques put out in research articles between 2015 and 2020, arranged in a table of comparisons. The study concluded with advantages and dis-advantages of DNNs in identifications of brain tumours [11].

Qasem et al. [10] proposes an MRI and Computed Tomography (CT) brain scans for brain tumour detection, favouring MRI for its lower risk. We applied the watershed segmentation technique, with the methodology divided into preprocessing, foreground computation using watershed, and feature extraction for ML algorithms. The approach was tested on a large dataset where K-Nearest Neighbours (KNNs) based classifications were satisfactory in brain tumour detections [12]. Solanki et al. [11] various techniques for identifying brain tumours and cancers, including an evaluation matrix for various datasets and platforms. Brain tumour morphology, accessible datasets, augmentation methods, feature extraction, and classification utilizing ML, DL, and TL models are all covered. The paper also consolidates information on tumor identification, detailing the benefits, limitations, advancements, and future trends in the field [13].

Khairandish et al. [12] evaluated according to performance, suggested model, dataset, and method type. These studies' accuracy scores varied from 79% to 97.7%. The most prevalent algorithms, in order of frequency, were CNN, KNN, C-means, and Random Forest (RF). Although the methodologies produced promising findings, there is still potential for improvement in the accuracy of brain tumour detection. Developments of software applications in these domains help improve practical solutions [14].

Alsaif et al. [13] reviewed architectures of CNNs including VGG, ResNets, and AlexNets. The study also discusses effective methods for detecting brain cancers from MRI datasets using CNNs and data augmentations where assessments showed their suggested approach outperformed other results by obtaining high detection accuracy and excelling in deep architectural design [15].

Jabbar et al. [14] investigated architectures of CNNs emphasizing on models including VGG, AlexNets, and ResNets along with successful strategies for detecting brain tumours on MRI datasets that incorporated CNNs and data augmentations. Their suggested approach showed considerable enhancements in detection accuracies in assessments with deep architectural designs [16].

Rajan and Sundar [15] employed Fuzzy C-Means (KMFCM) with active contour by level sets and K-means clusters for efficient brain tumours segmentations. Their method improved segmentations, edge detections, and intensities benefitting tumour diagnostics. Their dynamic contour and level set techniques provided precise segmentations. Their assessments were on processing times, detected tumour areas, and white/black pixel counts. The study segmentate complex areas efficiently and successfully. Tumour dimensions were utilized to assess accuracy, sensitivity, specificity, and similarity indices. Tumour volumes were also computed, giving doctors important information for diagnostic and therapy plans [17].

Tumour classifications by Thayumanavan and Ramasamy [16] involved preprocesses, feature extractions, classifications, and segmentations on T1-weighed MRI brain images. Median filters maximized skull stripping in MRI images, improving extractions of aberrant brain tissues in low contrast areas and accurately delineating damaged borders. Histogram of Oriented Gradients (HOG) and Discrete Wavelet Transform (DWT) extracted features with the former working on textural and shape data. Random Forest Classifiers (RFC), Support Vector Machine (SVM), and Decision Trees (DTs) classified samples where enhanced values for sensitivity, specificity, and accuracy were obtained [18].

According to Vankdothu et al. [17], CNN feature extractions were enhanced by the combination of CNNs with LSTM networks where LSTM-CNN architectures outperformed conventional CNNs in classifications. The suggested approach performed better than Recurrent Neural Network (RNN) models in terms of

accuracies on Kaggle dataset of 3,264 MRI samples with 2,870 training and 394 test images. Their results indicated the hybrid LSTM-CNN greatly enhanced classification performances [19].

Sajid et al. [18], used DL for brain tumour segmentations on a variety of MRI modalities. Their hybrid CNNs predicted output labels using both local and contextual information. While a two-phase training approach tackles data imbalance, dropout regularization and batch normalization combat overfitting. A CNN feed-forward pass and post-processing are used to remove minor false positives close to the skull after preprocessing procedures for image normalization and bias field correction. The approach outperforms current methods with dice scores, sensitivity, and specificity of 0.86, 0.86, and 0.91, respectively, as demonstrated by validation on the BraTS 2013 dataset [20].

3 | Proposed Methodology

The hybrid DL approach is proposed in this study for better brain tumour classifications. The three main steps of the proposed method are preprocessing, feature selection, and classification. The general block diagram of the suggested system is shown in *Fig. 1*.

3.1 | Input Dataset Collection

The Brain Tumor Segmentation (BraTS) Challenge offers datasets focused on brain tumor analysis, primarily using structural MRI modalities like T1, T1Gd, T2, and Fluid Attenuated Inversion Recovery (FLAIR). Some versions also include DCE-MRI sequences, which provide additional detail by capturing contrast agent dynamics, crucial for tumor vascular characterization. These datasets are meticulously annotated with tumor sub-regions, aiding in model training for tumor detection and classification. Researchers can benchmark their algorithms using metrics like Dice score, sensitivity, and specificity. BraTS datasets are vital for developing robust, accurate diagnostic tools in brain tumour analysis *(Fig. 2)* [21].

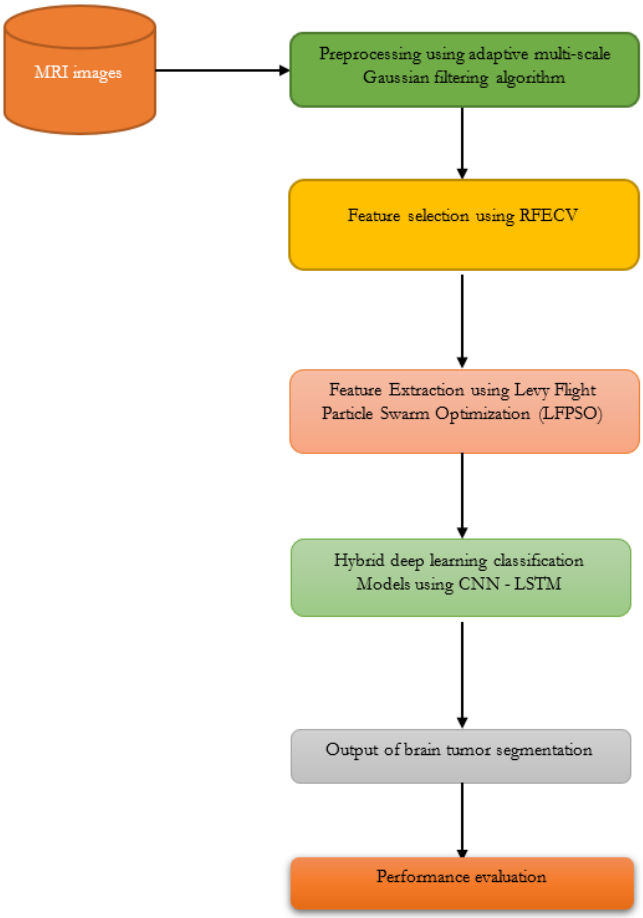

Fig. 1. Overall block diagram of brain tumour prediction.

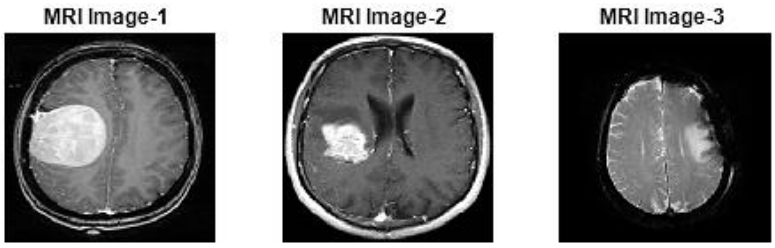

Fig. 2. Input images for brain tumour prediction.

3.2 | Pre-Processing Using Adaptive Multi-Scale Gaussian Filtering Algorithm

In this study, the AMGF algorithm method is employed for pre-processing to improves detection accuracy and speed, achieving an accuracy, sensitivity, specificity, Dice Similarity Coefficient (DSC) with processing times averaging with seconds [22].

Based on this paper, the AMGF is an image processing technique that dynamically adjusts the Gaussian filter's variance (σ^2) based on local image characteristics, enhancing image quality by addressing challenges like noise suppression and edge preservation. The two-dimensional Gaussian filter is expressed in *Eq. (1)*.

$$G(x,y) = \frac{1}{2\pi\sigma^2}\exp\left(-\frac{(x^2+y^2)}{2\sigma^2}\right), \quad (1)$$

G (x, y) is the Gaussian filter function, σ^2 is the variance, and x and y are pixel coordinates. Filter kernel sizes are typically set by values greater than 5% of the kernel's maximum value. Traditional Gaussian filtering, while efficient for noise reduction, can blur key features and create edge displacement, disappearing edges, and phantom edges, particularly when pixel intensity varies quickly.

AMGF addresses these difficulties using two primary strategies:

I. Multi-scale filtering: the image is pre-processed using Gaussian filters with different variances, capturing both fine and broad features. This enables a synthesis of data that balances noise reduction with edge retention. Adaptive

II. Variance: the filter variance is modified based on local image properties (e.g., noise level, edge type), ensuring that image fragments are smoothed according to individual needs.

Mathematically, Gaussian filtering of signals $F(x)$, abbreviated as $F_z(x)$, is represented as *Eq. (2)*.

Gaussian filters can be expressed mathematically as *Eq. (2)*.

$$F_z(x) = F(x) + \frac{\sigma^2}{2}F''(x) + \text{higher\_order terms}, \quad (2)$$

where $F''(x)$ signify second derivatives of $F(x)$.

Adaptive variances $\sigma^2(x,y)$ are depicted in *Eq. (3)*.

$$\sigma^2(x,y) = \frac{1}{F(x,y)}, \quad (3)$$

F (x, y) implies pixel brightness (intensities). Filters are matched to individual requirements conserving finer details with reduced noises.

A complex approach minimizes mean square errors E (σ) when fluctuations of pixel variance are less. Best variance filters can be obtained by minimizing errors and defined as *Eq. (4*).

$$E(\sigma) = ||G * F - F||^2 + \lambda\,||\nabla\sigma||^2, \quad (4)$$

where G represents Gaussian filters, F stands for images, ∗ implies convolutions while λ are regularization parameters for limiting smoothness of variances. AMGF can be effective on MRI images as they emphasize important traits while reducing noises, thus assisting in detections of edges, segmentations and feature extractions (*Fig. 3*).

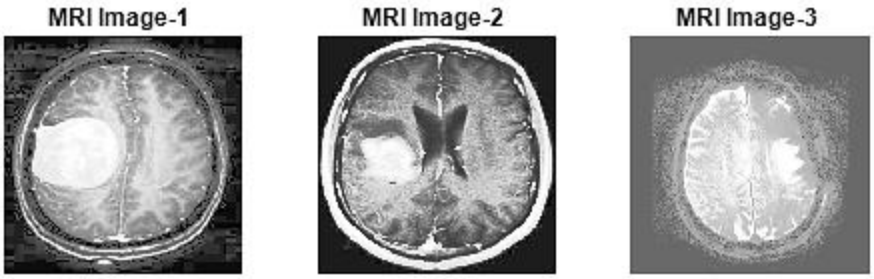

Fig. 3. Pre-processed images for brain tumour prediction.

Algorithm 1. AMGF algorithm.

Pre-process the image with Gaussian filters of various σ^2 values (multi-scale filtering).
Calculate the local image attributes (such as intensity and contrast).
Adapt the Gaussian filter variance $\sigma^2(x, y)$ based on local factors.
Apply an adaptive Gaussian filter on the image.
To get the best filter variance for each pixel, minimize the error E (σ).
Combine the data from the various scales to get the final improved image.

AMGF enhance image qualities with dynamic modifications of Gaussian filter variance using local data. This flexibility, especially at borders where pixel intensity changes significantly, allows for good noise reduction while retaining crucial image information. The AMGF technique is beneficial for edge identification, segmentation, and feature extraction since it may change the filter variance for each pixel, increasing detection accuracy and processing efficiency [22].

3.3 | Feature Selection Using Recursive Feature Elimination with Cross-Validation Algorithm

This work's suggested RFECV schema selects features using ML method where wrappers are used in feature selections and determine important characteristics. By combining recursive feature reduction with cross-validation, it improves resilience by determining the ideal number of features that improve model performance. Each feature in RFECV is assessed by a classification model, and attributes that do not increase classification accuracy are progressively eliminated (*Fig. 4*). As explained in *Algorithm 2*, the method begins with the entire collection of characteristics and progressively eliminates irrelevant features to select the most advantageous feature subset. RFECV was used in this work using the DT model (DT-RFECV) with stratified fold splitting and a 10-fold cross-validation procedure to maintain the class distribution. Ten identically sized folds were created from the dataset [23].

To ascertain how feature removal affects model performance, the accuracy measure is calculated at each step of the recursive elimination process. The importance and contribution of each component are revealed through this iterative approach. The feature subset with the best overall accuracy is considered optimum. Following elimination processes, selected feature sets are validated using ten-fold cross-validation where folds serve as validation sets during DT model's training and testing cycles. Measurements of accuracies assess model's resilience and ability to generalize new data. Thorough evaluations of performances are given by averages and Standard Deviations (STDs) of accuracy measures across ten iterations.

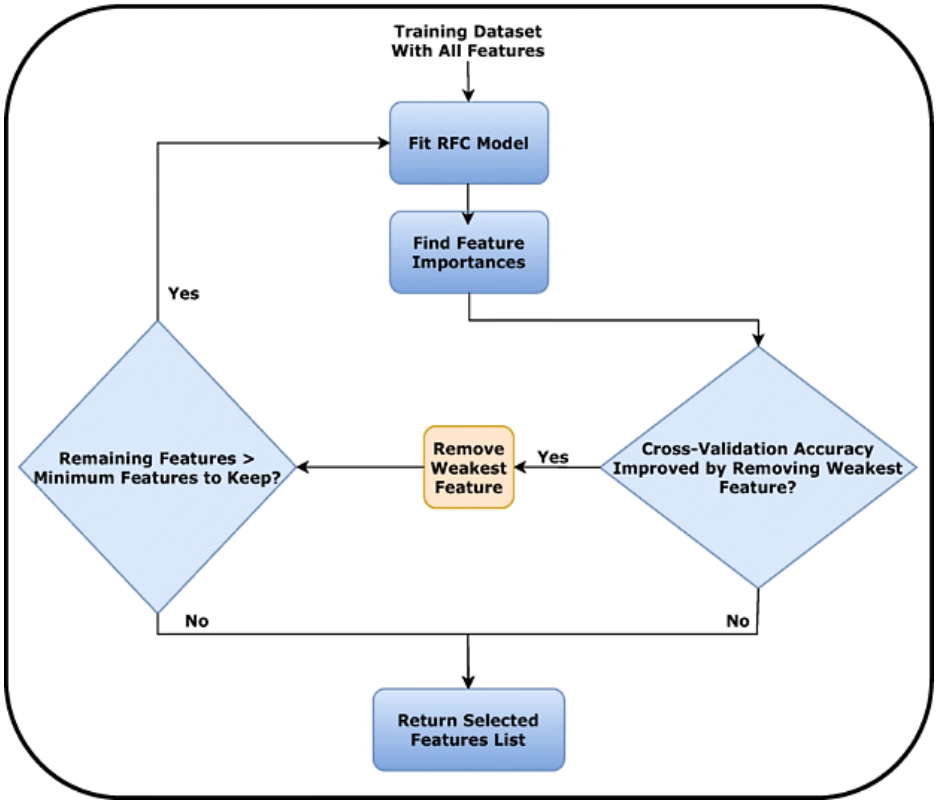

Fig. 4. RFECV flowchart model diagram.

Algorithm 2. RFECV algorithm.

Input: training dataset X
Output: ranked features

I. For each feature in datasets X:
II. For $k = 1$ to 10 (where k is cross-validation fold count):
   - Using Stratified K-Fold technique, randomly divide datasets X into 10 equal subgroups.
   - Make use of nine subsets as training sets and one subset as validation sets.
   - Use training data to train classification models.
   - Using validation data, determine model's prediction accuracy.
   - Determine each feature's significance based on the model's assessment.
   - Update the training data and eliminate the least significant characteristics.
III. Identify the feature subset FS that achieves the highest prediction accuracy.
IV. If FS has the highest prediction accuracy:
V. Mark FS as the selected features.
VI. Return the ranked list of selected features.

Information on RFECV [24] is included in *Algorithm 2*, which facilitates a comprehensive assessment of feature importance and helps create a more accurate and widely applicable model. RFECV improved intrusion detection feature selection thanks to the selected feature set's improved performance and generalization to previously unidentified data. All things considered, RFECV is a sound and trustworthy technique for improving feature sets, producing more precise and dependable models for intrusion detection and other uses.

3.2 | Feature Extraction Using Lévy Flight Particle Swarm Optimization

LFPSO [25] allows swarms to explore more efficiently by including Lévy flights into Particle Swarm Optimizations (PSO). The combination is especially useful in challenging optimization scenarios like brain tumour detections since it improves feature choices, parameter modifications, and other crucial processes. Lévy flights, which are random walk methods with heavy-tailed distributions, are used into LFPSO to improve

global exploration and prevent local optima in PSO frameworks. By using these features, LFPSO enhances PSO's performance in complex search domains. Every particle in LFPSO has a location (X_i) and a velocity (V_i). *Eq. (5)* and *Eq. (6)* update particle locations and velocities in the manner shown below:

$$V_i(t+1) = \omega \,.\, V_i(t) + c_1 \,.\, r_1 . \left(\rho_{best,i} - X_i\right) + c_2 \,.\, r_2 . (g_{best} - X_i). \quad \textbf{(5)}$$

$$X_i(t+1) = X_i(t) + V_i(t+1). \quad \textbf{(6)}$$

Here, ω is the inertia weight, c_1 and c_2 are acceleration coefficients, r_1 and r_2 are random numbers in [0,1], $\rho_{best,i}$ implies best positions of particles i , g_{best} represents global best positions.

The Lévy flight mechanism modifies the standard particle movement. A random vector L drawn from a Lévy distribution is used to update the particle's position in *Eq. (7)* as follows.

$$X_{new} = X + \alpha \,.\, L. \quad \textbf{(7)}$$

In this, L represents the Lévy flight step size, which is typically generated from a Lévy distribution in *Eq. (8)*.

$$(\lambda) = \frac{u}{|v|\, 1/\lambda}, \quad \textbf{(8)}$$

where u and v are random variables drawn from normal distributions, and λ is the Lévy flight exponent, usually set to 1.5. The LFPSO algorithm begins with the initialization and considering a swarm of particles with arbitrary locations and speeds, and variables like Lévy flight parameters, acceleration coefficients, and inertia weight are established. Objective functions i.e. brain tumor detection accuracies are used to assess particles' fitnesses. Based on fitness assessments, the computer then modifies the global best and personal best locations for every particle. The Lévy flight update step involves generating a random step size from the Lévy distribution and updating each particle's position in *Eq. (9)*.

$$X_i(t+1) = X_i(t) + \alpha \,.\, L. \quad \textbf{(9)}$$

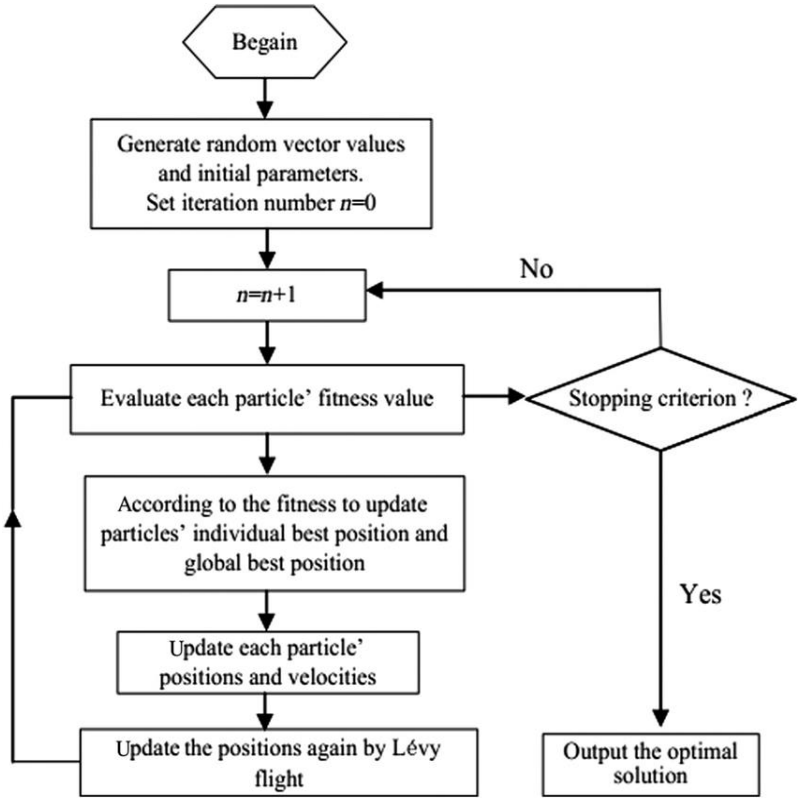

Fig. 3. Flowchart of the Lévy Particle Swarm Optimization (LPSO) algorithm.

The LFPSO training procedure [26] can be used to improve image preprocessing steps to improve image quality prior to feature extractions, optimize feature selections to find most informative features for classifications, and adjust parameters of ML models such as SVM or CNN to improve performances. LFPSO can increase the precision and resilience of brain tumour detection models by using Lévy flight's exploring capabilities.

3.5|Classification Using Hybrid Deep Learning Classification Models with Convolutional Neural Network-Long Short-Term Memory

In medical imaging, brain tumour identification [27] is a crucial endeavour, and precise categorization is essential for patient care and outcome. CNNs and LSTMs are combined to create a strong hybrid DL model that capitalizes on the advantages of both architectures. While LSTMs are excellent at capturing temporal connections, CNNs are skilled at extracting spatial characteristics. The hybrid CNN-LSTM model is examined in this section. for brain tumour detection, presenting key formulas, equations, and the algorithmic approach.

3.5.1|Convolutional neural network-long short-term memory hybrid model architecture

The hybrid model starts with CNNs [28], which use convolutional, pooling, and fully connected layers to effectively capture spatial hierarchy in images. When an input image X has dimensions $H \times W \times D$, where L is the depth or channel count, B is the height, and W is the width, the convolution operation applies a filter F of size $f_h \times f_w \times D$ to produce an output feature map Y in *Eq. (10)*.

$$Y_{i,j,k} = \sum_{h=1}^{f_h} \sum_{w=1}^{f_w} \sum_{d=1}^{D} X_{i+h-1,j+w-1,d} \cdot F_{h,w,d,k}. \quad (10)$$

Here, k represents the k k-th filter, and i, j are spatial indices.

To introduce non-linearity, the Rectified Linear Unit (ReLU) is applied element-wise in *Eq. (11)*.

$$\mathrm{ReLU}(x) = \max(0, x). \quad (11)$$

Max Pooling reduces spatial dimensions of feature maps as per *Eq. (12)*.

$$Y_{i,j,k} = \max\left(X_{2i-1:2i,2j-1:2j,k}\right). \quad (12)$$

LSTMs, a kind of RNNs represent long-term dependencies in sequential data. In addition to input (it), forget (ft), and output (OT) gates, LSTM units include memory cells (Ct) that maintain cell states.

The forget gate operation is defined as *Eq. (13)*:

$$f_t = \sigma(W_f . [h_{t-1}, x_t] + b_f. \quad (13)$$

The input gate is defined as *Eq. (14)*:

$$i_t = \sigma(W_i . [h_{t-1}, x_t] + b_i. \quad (14)$$

The cell state is updated as follows *Eq. (15):*

$$c_t = f_t \odot c_{t-1} + i_t \odot \tan h\,(W_c . [h_{t-1}, x_t] + b_c. \quad (15)$$

The output gate is defined as *Eq. (16)*:

$$o_t = \sigma(W_o . [h_{t-1}, x_t] + b_o. \quad (16)$$

Finally, the hidden state is given by *Eq. (17)*:

$$h_t = o_t \odot \tan(c_t). \quad (17)$$

Here, σ represents the sigmoid activation function, $\odot$ denotes element-wise multiplication, are weight matrices, W_f, W_i, W_c, W_o and b_f, b_i, b_c, b_o are biases. The CNN-LSTM hybrid model combines the ability of

CNNs to extract spatial features with the capability of LSTMs to describe temporal dependencies. The CNN's feature maps are usually sent into the LSTM network as part of the design. Given an input MRI image I with dimensions $H \times W \times D$, the process begins with CNN-based feature extraction *Eq. (18)*;

$$F_{cnn} = CNN(I), \quad \textbf{(18)}$$

here, F_{cnn} represents the feature map extracted by the CNN, which is a 3D tensor. F_{cnn} is then reshaped into a 2D matrix suitable for LSTM input (*Eq. 19*);

$$F_{lstm-in} = reshape(F_{cnn}). \quad \textbf{(19)}$$

The LSTM processes the reshaped features to model temporal dependencies (*Eq. 20*);

$$h_t = LSTM(F_{lstm-in}). \quad \textbf{(20)}$$

Finally, classification is performed using a SoftMax function (*Eq. 21*);

$$y_{pred} = SoftMax(W_h . h_t + b_h), \quad \textbf{(21)}$$

where W_h and b_h are weights and biases associated with the final fully connected layer, and y_{pred} represents the predicted probabilities for each tumor class.

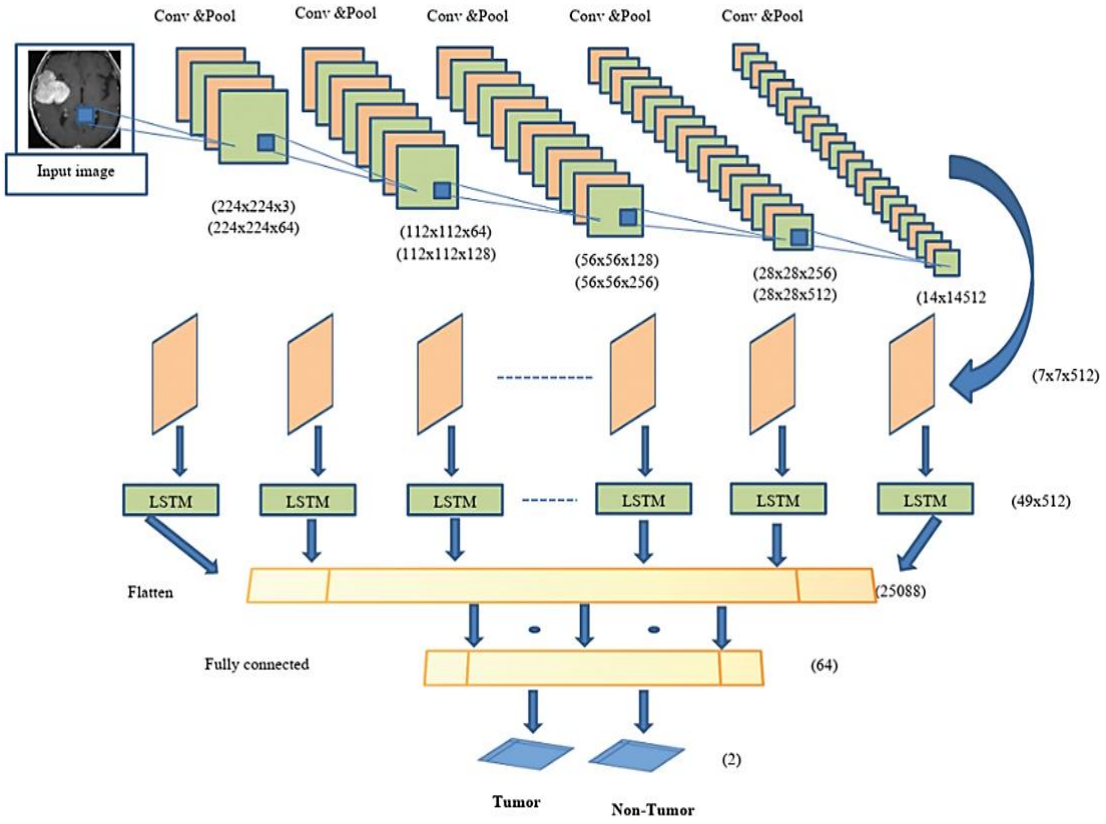

Fig. 4. Structure of proposed hybrid CNN-LSTM.

The temporal sequence modelling powers of LSTMs and the spatial feature extraction skills of CNNs are successfully combined in the hybrid CNN-LSTM model [29]. This hybrid method works especially well for detecting brain tumours, where contextual and spatial information are both essential. By following the outlined algorithm and utilizing the defined equations, the model can achieve high accuracy in classifying brain tumours from MRI images. *Figs. 5* and *6* described the classification of images in MATLAB screens. The architecture can be further enhanced by incorporating advanced techniques such as attention mechanisms, TL, or more sophisticated CNN and LSTM architectures.

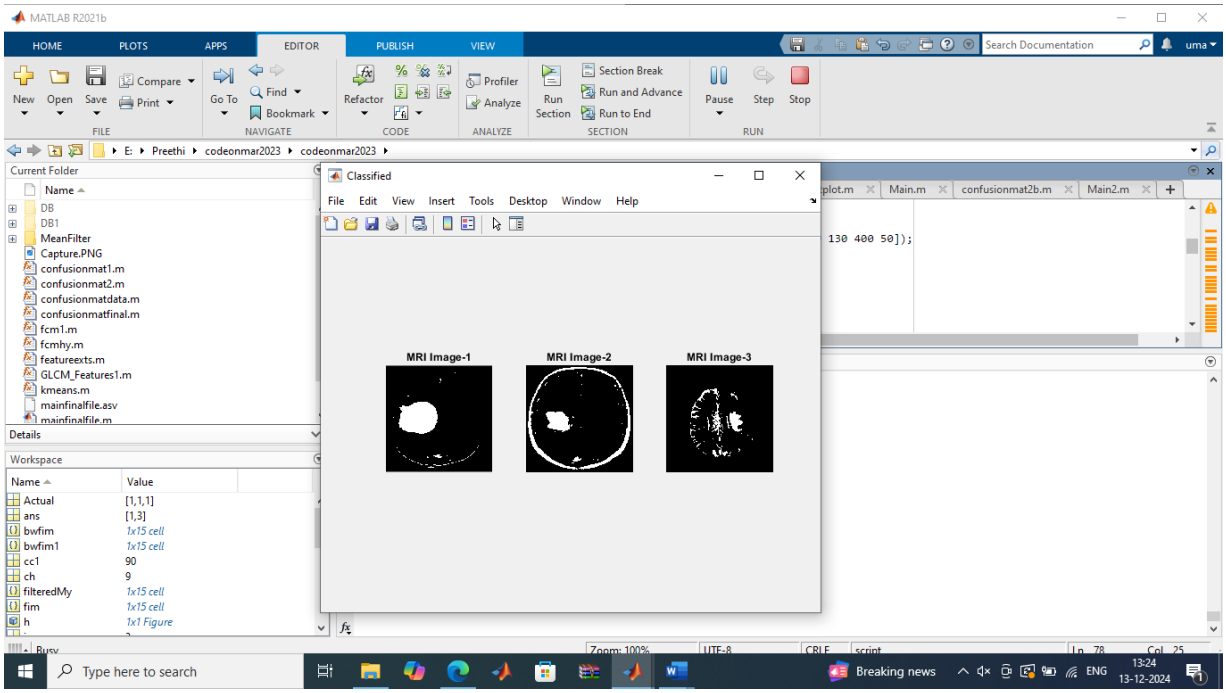

Fig. 5. MATLAB implementation classification screen.

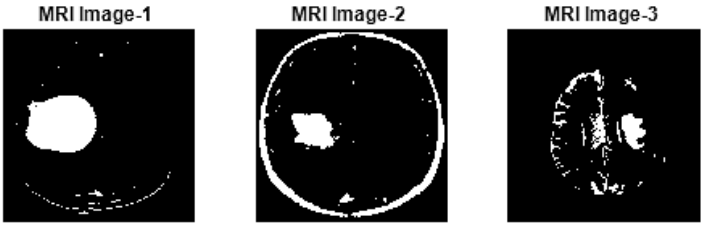

Fig. 6. Final classified images in matlab.

4 | Experimental Result

In this part [30], we used the BraTS Challenge datasets, which were created exclusively for brain tumour analysis with structural MRI modalities such as T1, T1Gd, T2, and FLAIR. Some of these datasets contain DCE-MRI sequences. These sequences give detail by capturing contrast agent dynamics, which are necessary for characterizing tumour vasculature. These properly annotated datasets with tumour sub-regions serve as crucial ground truths for training models during detections and classifications of tumour samples. CNN-LSTM hybrid model in comparison to other methods performs better on metrics including sensitivity, specificity, and Dice scores, thus proving dependability of diagnostics[1]. These data form a crucial foundation for developing better models for detecting brain tumors. The results of performance comparisons with various techniques and our suggested CNN-LSTM hybrid model are provided. Skewness, kurtosis, entropy, mean, and STD are the five primary metrics used to evaluate segmentation performance. Each aspect offers a fresh perspective on the image's qualities.

[1] BraTS Challenge datasets are available at https://www.kaggle.com/datasets/dschettler8845/brats-2021-task1

4.1 | Mean

Mean values in brain MRI refer to average pixel intensities in images. Pixel values are added together and results divided by complete pixel counts, expressed mathematically as *Eq. (22)*;

$$\text{Mean} = \frac{1}{m \times n} \sum_{i=0}^{m-1} \sum_{j=0}^{n-1} I(i,j), \tag{22}$$

where m and n are the image dimensions.

4.2 | Standard Deviation

The STD, which reflects the image's contrast and homogeneity, quantifies the distribution of pixel values around the mean in brain MRIs. In *Eq. (23)* it is computed as the variance's square root;

$$\text{STD}(\sigma) = \sqrt{\frac{1}{m \times n} \sum_{i=0}^{m-1} \sum_{j=0}^{n-1} (I(i,j) - M)^2}, \tag{23}$$

where M is the mean pixel value.

4.3 | Entropy

Entropies in *Eq. (24)* are degrees of unpredictability or randomness in image textures, and indicate necessary information for characterizing distributions of pixel intensities in brain MRIs, Greater entropy levels imply complex textures and lower values imply uniform textures.

$$\text{Entropy} = -\sum_{i=0}^{m-1} \sum_{j=0}^{n-1} f(i,j) \log 2 \big(f(i,j)\big). \tag{24}$$

4.4 | Kurtosis

Kurtosis quantifies the existence of outliers and the form of the pixel intensity distribution in the context of brain MRI. It helps in understanding the distribution's peakedness or flatness compared to a normal distribution in *Eq. (25)*;

$$\text{Kurtosis} = \frac{\frac{1}{m \times n} \sum_{i=0}^{m-1} \sum_{j=0}^{n-1} (f(i,j) - M)^4}{(\text{STD})^4}, \tag{25}$$

where $F(i,j)$ represents pixel intensity and M is the mean.

4.5 | Skewness

In the context of brain MRI, Skewness measures the asymmetry of pixel intensity distribution. It indicates whether the pixel values are more concentrated on one side of the mean in *Eq. (26)*;

$$\text{Skewness} = \frac{\frac{1}{m \times n} \sum_{i=0}^{m-1} \sum_{j=0}^{n-1} (f(i,j) - M)^3}{(\text{STD})^3}, \tag{26}$$

where STD is the standard deviation.

Table 1. performance analysis of segmentation model of brain tumour.

Image Types	Mean	STD	Entropy	Kurtosis	Skewness
Meningiomas tumor images	0.0051	0.100	3.38	36.32	5.96
Gliomas tumor images	0.0050	0.099	3.13	34.23	5.87
Pituitary tumors image	0.0052	0.098	3.11	33.12	5.81
Medulloblastomas tumor images	0.0051	0.099	3.25	34.75	5.90

4.6 | Accuracy

In the context of brain MRI [31], accuracy is a metric that reflects the overall correctness of the model's predictions regarding true pixels. It is calculated as the proportion of correctly predicted true pixels. The *Eq. (27)* for accuracy is:

$$\text{Accuracy (AC)} = \frac{\text{TP} + \text{TN}}{\text{TP} + \text{FP} + \text{TN} + \text{FN}} \tag{27}$$

In this case TP would be a true positive, TN would be a true negative, FP would be a false positive, and FN would be a false negative.

Table 2. Results of performance comparison.

Metrics	Methods						
	KNN	SOM	GA	GCNN	Kernel-Based SVM	ICA-CNN-SVM	DCA-CNN-LSTM
Accuracy	0.85	0.92	0.98	0.96	0.98	0.989	0.991
Sensitivity	0.39	0.43	0.51	0.85	0.98	0.99	0.993
Specificity	0.42	0.52	0.54	0.89	0.98	0.99	0.993
DSC	0.81	0.83	0.85	0.89	0.94	0.981	0.985
Executive time	3.7s	4.8s	2.8s	0.92s	0.83s	0.43s	0.38s

The accuracy of seven models in brain tumor detection is compared in the performance analysis graph shown in *Fig. 5*. The Dual Cross Attention (DCA)-CNN-LSTM model leads with an accuracy of 99.1%, followed by Independent Component Analysis (ICA)-CNN-SVM at 98.9%. Genetic Algorithm (GA) and Kernel-based SVM both achieve 98%, while Graph Convolutional Neural Network (GCNN) scores 96%. Self-Organizing Map (SOM) and KNN lag behind with 92% and 85% accuracy, respectively.

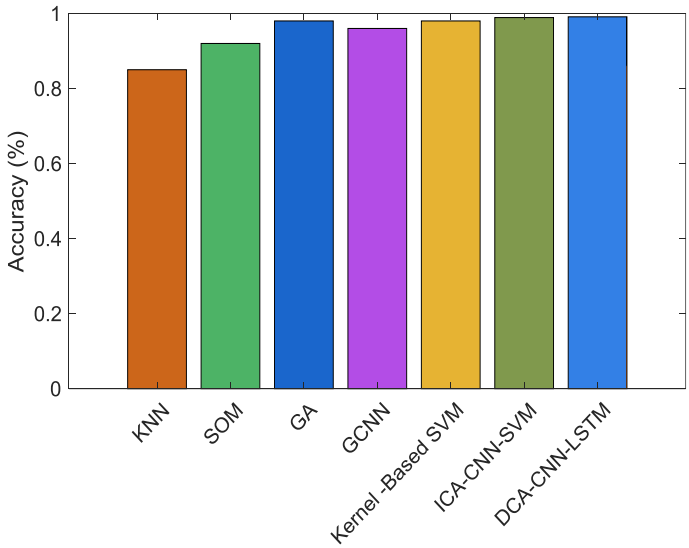

Fig. 5. Accuracy of the methods.

4.7 | Sensitivity

Sensitivity in brain MRI refers to the precision of detecting pixels that are part of positive classifications. It measures how well a model can identify good examples. According to *Eq. (28)* sensitivity is defined as the ratio of real positive pixels to all pixels classified as positive. The True Positive Rate (TPR) is another name for sensitivity [32]. The sensitivity equation is

$$\text{Sensitivity} = \frac{\text{TP}}{\text{TP} + \text{FN}}. \tag{28}$$

In *Fig. 6*, The sensitivity of seven models in brain tumor detection is compared in the performance analysis graph. The DCA-CNN-LSTM model demonstrates the highest sensitivity at 99.3%, closely followed by ICA-CNN-SVM with 99%. Kernel-based SVM achieves 98%, while GCNN reaches 85%. In contrast, the GA, SOM, and KNN models exhibit lower sensitivity levels, with values of 51%, 43%, and 39%, respectively. This comparison highlights the superior ability of the DCA-CNN-LSTM model to correctly identify true positive cases in brain tumor detection, outperforming the other models.

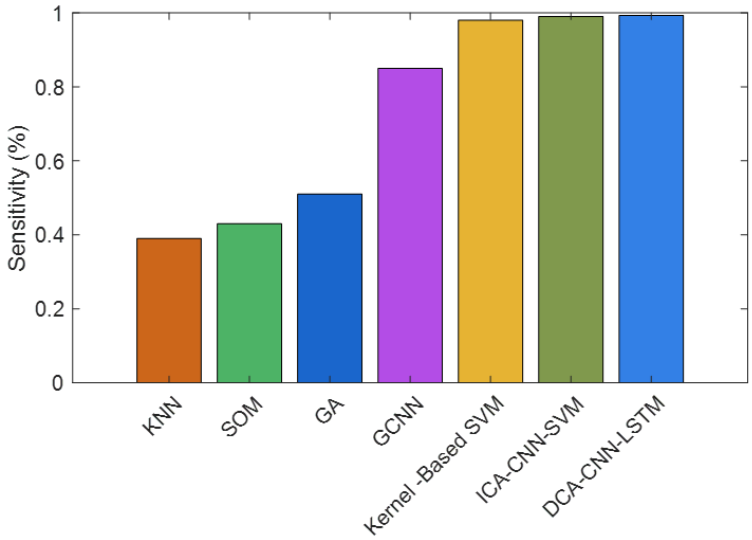

Fig. 6. Sensitivity of the methods.

4.8 | Specificity

The ability to accurately identify pixels that correspond to negative classes is measured by specificity in brain MRI imaging [33]. It measures how well a model can identify negative examples. According to *Eq. (29)*, specificity is determined by dividing the total number of pixels recognized as negative by the ratio of real negative pixels. Another name for specificity is the True Negative Rate (TNR). The specificity *Eq. (29)* is

$$\text{Specificity} = \frac{\text{TN}}{\text{TN} + \text{FP}}. \tag{29}$$

From the *Fig. 7*, The specificity of seven models in brain tumor detection is evaluated in the performance analysis graph. The DCA-CNN-LSTM model achieves the highest specificity at 99.3%, closely followed by ICA-CNN-SVM with 99%. The Kernel-based SVM model also performs well, reaching 98% specificity, while the GCNN model records a specificity of 89%. In contrast, the GA, SOM, and KNN models show lower specificity levels, with values of 54%, 52%, and 42%, respectively. This comparison underscores the DCA-CNN-LSTM model's superior capability to accurately identify true negative cases in brain tumor detection, significantly outperforming the other models.

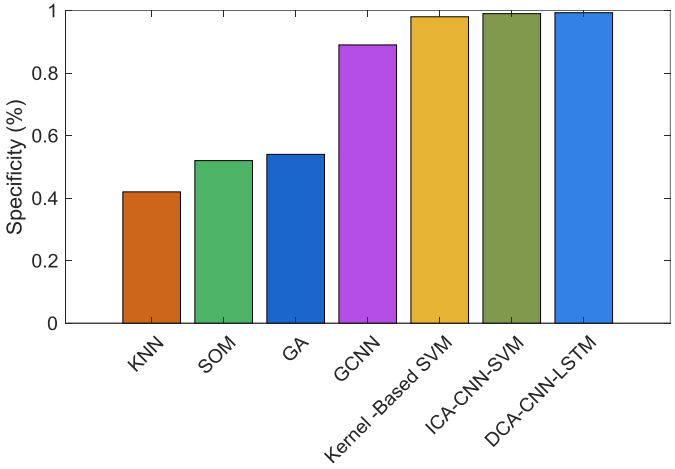

Fig. 7. Specificity results of the methods.

4.9 | Dice Similarity Coefficient

In brain MRI, the overlap between the actual ground truth and the projected output is measured by the DSC. It calculates the degree of similarity between the ground truth and anticipated areas. The genuine positive values are compared to the mean of the ground truth and anticipated values to determine the dice score [34]. The Dice score's *Eq. (30)* is

$$\mathrm{DSC} = \frac{2 \times \mathrm{TP}}{2 \times \mathrm{TP} + \mathrm{FN} + \mathrm{FP}}. \tag{30}$$

In the *Fig. 8*, The DSC of seven models in brain tumor detection is evaluated in the performance analysis graph. The DCA-CNN-LSTM model stands out with the highest DSC of 0.993, indicating excellent alignment between predicted and actual tumor regions. The DSC of 0.98 is attained by the Kernel-Based SVM model, while the ICA-CNN-SVM model comes in second with a DSC of 0.99. With a DSC of 0.89, the GCNN model performs admirably as well. With DSC values of 0.54, 0.52, and 0.42, respectively, the GA, SOM, and KNN models were in contrast. This comparison shows that the DCA-CNN-LSTM model outperforms the other models by a significant margin in terms of accurately segmenting brain tumours.

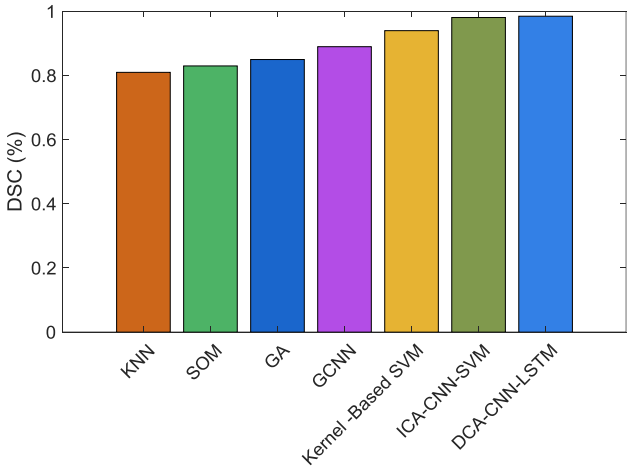

Fig. 8. DSC.

4.10 | Execution Time

In the case of brain MRI, the execution time has a significant impact on the model's efficacy [35]. The time it takes for the model to process an image and provide a result is indicated. The model's computation

performance is shown by the execution time, which is measured in milliseconds or seconds. In reality, the following *Eq. (25)* may be used to determine execution time T;

$$\mathrm{T} = \text{End Time} - \text{Start Time},$$

where the timestamps recorded at the conclusion and beginning of the model's processing phase are denoted by the End Time and Start Time, respectively. This statistic helps determine how to balance computer efficiency and accuracy in brain tumour detection efforts. Based on *Fig. 8* The DCA-CNN-LSTM model performs better than the others when comparing execution times for various brain tumour detection models, requiring just 0.38 seconds. The ICA-CNN-SVM model, which executes in 0.43 seconds, comes next. The GCNN model runs in 0.92 seconds, whereas the Kernel-based SVM model does so in 0.83 seconds. At 3.7 and 4.8 seconds, respectively, the KNN and SOM models executed considerably more slowly. Compared to the other models, the GA model exhibits slower processing and greater unpredictability, with execution durations ranging from 2.8 to 5 seconds. All things considered, the accuracy and processing speed of the DCA-CNN-LSTM model are excellent.

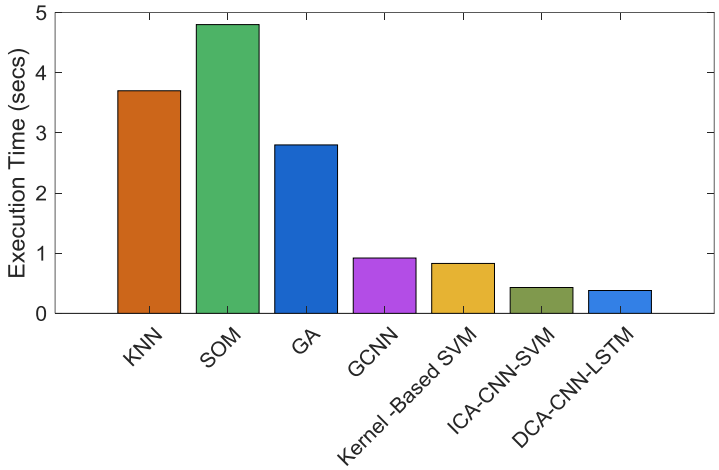

Fig. 8. Execution Time the algorithms.

5 | Conclusion

In conclusion, our study suggested a novel brain tumour detection framework that combines sophisticated preprocessing techniques with a hybrid DL methodology. The technology uses AMGF in combination with DCE-MRI to significantly increase image quality and minimize noise. Lévy LFPSO is used for detailed feature extraction, whereas RFECV is used for precise feature selection. When CNNs and LSTMs are integrated, both temporal and spatial patterns are caught, resulting in high classification accuracy. The approach yields remarkable performance metrics 0.991 accuracy, 0.993 sensitivity and specificity, and a DSC of 0.985 while being efficient at 0.38 seconds. This new framework displays considerable improvements in brain tumour detections, providing reliable and economical solutions for better patient outcomes in clinical practices.

Data Availability

All data are included in the text.

Funding

No external funding was received for this research.

Conflict of Interest

The authors declare no conflict of interest.

References

[1] Babu Vimala, B., Srinivasan, S., Mathivanan, S. K., Mahalakshmi, Jayagopal, P., & Dalu, G. T. (2023). Detection and classification of brain tumor using hybrid deep learning models. *Scientific reports*, *13*(1), 1-17. https://doi.org/10.1038/s41598-023-50505-6

[2] Kanchanamala, P., K.G., R., & Ananth, M. B. J. (2023). Optimization-enabled hybrid deep learning for brain tumor detection and classification from MRI. *Biomedical signal processing and control*, *84*, 104955. https://doi.org/10.1016/j.bspc.2023.104955

[3] Deb, D., & Roy, S. (2021). Brain tumor detection based on hybrid deep neural network in MRI by adaptive squirrel search optimization. *Multimedia tools and applications*, *80*(2), 2621–2645. https://doi.org/10.1007/s11042-020-09810-9

[4] Raza, A., Ayub, H., Khan, J. A., Ahmad, I., S. Salama, A., Daradkeh, Y. I., …, & Hamam, H. (2022). A hybrid deep learning-based approach for brain tumor classification. *Electronics*, *11*(7), 1-17. https://doi.org/10.3390/electronics11071146

[5] Shanthi, S., Saradha, S., Smitha, J. A., Prasath, N., & Anandakumar, H. (2022). An efficient automatic brain tumor classification using optimized hybrid deep neural network. *International journal of intelligent networks*, *3*, 188–196. https://doi.org/10.1016/j.ijin.2022.11.003

[6] Sudharson, K., Sermakani, A. M., Parthipan, V., Dhinakaran, D., Petchiammal, G. E., & Usha, N. S. (2022). Hybrid deep learning neural system for brain tumor detection. *2022 2nd international conference on intelligent technologies (CONIT)* (pp. 1–6). IEEE. https://doi.org/10.1109/CONIT55038.2022.9847708

[7] Munir, K., Frezza, F., & Rizzi, A. (2022). Deep learning hybrid techniques for brain tumor segmentation. *Sensors*, *22*(21), 1–26. https://doi.org/10.3390/s22218201

[8] Sindhiya Devi, R., Perumal, B., & Pallikonda Rajasekaran, M. (2022). A hybrid deep learning based brain tumor classification and segmentation by stationary wavelet packet transform and adaptive kernel fuzzy c means clustering. *Advances in engineering software*, *170*, 103146. https://doi.org/10.1016/j.advengsoft.2022.103146

[9] Nazir, M., Shakil, S., & Khurshid, K. (2021). Role of deep learning in brain tumor detection and classification (2015 to 2020): A review. *Computerized medical imaging and graphics*, *91*, 101940. https://doi.org/10.1016/j.compmedimag.2021.101940

[10] Qasem, S. N., Nazar, A., Qamar, A., Shamshirband, S., & Karim, A. (2019). A learning based brain tumor detection system. *Computers, materials & continua*, *59*(3), 713-727. https://doi.org/10.32604/cmc.2019.05617

[11] Solanki, S., Singh, U. P., Chouhan, S. S., & Jain, S. (2023). Brain tumor detection and classification using intelligence techniques: An overview. *IEEE access*, *11*, 12870–12886. https://doi.org/10.1109/ACCESS.2023.3242666

[12] Khairandish, M. O., Sharma, M., & Kusrini, K. (2020). The performance of brain tumor diagnosis based on machine learning techniques evaluation-a systematic review. *2020 3rd international conference on information and communications technology (ICOIACT)* (pp. 115–119). IEEE. https://doi.org/10.1109/ICOIACT50329.2020.9332131

[13] Alsaif, H., Guesmi, R., Alshammari, B. M., Hamrouni, T., Guesmi, T., Alzamil, A., & Belguesmi, L. (2022). A novel data augmentation-based brain tumor detection using convolutional neural network. *Applied sciences*, *12*(8), 1–16. https://doi.org/10.3390/app12083773

[14] Jabbar, A., Naseem, S., Mahmood, T., Saba, T., Alamri, F. S., & Rehman, A. (2023). Brain tumor detection and multi-grade segmentation through hybrid caps-VGGNet model. *IEEE access*, *11*, 72518–72536. https://doi.org/10.1109/ACCESS.2023.3289224

[15] Rajan, P. G., & Sundar, C. (2019). Brain tumor detection and segmentation by intensity adjustment. *Journal of medical systems*, *43*(8), 282. https://doi.org/10.1007/s10916-019-1368-4

[16] Thayumanavan, M., & Ramasamy, A. (2021). RETRACTED: An efficient approach for brain tumor detection and segmentation in MR brain images using random forest classifier. *Concurrent engineering*, *29*(3), 266–274. https://doi.org/10.1177/1063293X211010542

[17] Vankdothu, R., Hameed, M. A., & Fatima, H. (2022). A brain tumor identification and classification using deep learning based on CNN-LSTM method. *Computers and electrical engineering*, *101*, 107960. https://doi.org/10.1016/j.compeleceng.2022.107960

[18] Sajid, S., Hussain, S., & Sarwar, A. (2019). Brain tumor detection and segmentation in MR images using deep learning. *Arabian journal for science and engineering*, *44*(11), 9249–9261. https://doi.org/10.1007/s13369-019-03967-8

[19] Menze, B. H., Jakab, A., Bauer, S., Kalpathy-Cramer, J., Farahani, K., Kirby, J., …, & Van Leemput, K. (2015). The multimodal brain tumor image segmentation benchmark (BRATS). *IEEE transactions on medical imaging*, *34*(10), 1993–2024. https://doi.org/10.1109/TMI.2014.2377694

[20] Sun, X., & Sun, X. F. (2024). An edge detection algorithm based upon the adaptive multi-directional anisotropic gaussian filter and its applications. *The journal of supercomputing*, *80*(11), 15183–15214. https://doi.org/10.1007/s11227-024-06044-6

[21] Deng, G., & Cahill, L. W. (1993). An adaptive gaussian filter for noise reduction and edge detection. *1993 IEEE conference record nuclear science symposium and medical imaging conference* (pp. 1615–1619 vol.3). IEEE. https://doi.org/10.1109/NSSMIC.1993.373563

[22] Kusrini, K., Yudianto, M. R. A., & Al Fatta, H. (2022). The effect of Gaussian filter and data preprocessing on the classification of Punakawan puppet images with the convolutional neural network algorithm. *International journal of electrical and computer engineering*, *12*(4), 3752-3761. https://doi.org/10.11591/ijece.v12i4.pp3752-3761

[23] Misra, P., & Yadav, A. S. (2020). Improving the classification accuracy using recursive feature elimination with cross-validation. *International journal on emerging technologies*, *11*(3), 659–665. https://www.researchgate.net/publication/344181117

[24] Awad, M., & Fraihat, S. (2023). Recursive feature elimination with cross-validation with decision tree: Feature selection method for machine learning-based intrusion detection systems. *Journal of sensor and actuator networks*, *12*(5), 1-23. https://doi.org/10.3390/jsan12050067

[25] Kołodziejczyk, J., & Tarasenko, Y. (2021). Particle swarm optimization and L´evy Flight integration. *Procedia computer science*, *192*, 4658–4671. https://doi.org/10.1016/j.procs.2021.09.244

[26] Deng, J., & Wang, Y. (2024). Application of Lévy flight particle swarm optimisation in MPPT of photovoltaic system. *International journal of electronics*, *111*(7), 1143–1162. https://doi.org/10.1080/00207217.2023.2210305

[27] Uyulan, C. (2020). Development of LSTM&CNN based hybrid deep learning model to classify motor imagery tasks. *Communications in mathematics and biology and neuroscience*. https://doi.org/10.28919/cmbn/5265

[28] Khademi, Z., Ebrahimi, F., & Kordy, H. M. (2022). A transfer learning-based CNN and LSTM hybrid deep learning model to classify motor imagery EEG signals. *Computers in biology and medicine*, *143*, 105288. https://doi.org/10.1016/j.compbiomed.2022.105288

[29] Suganthi, M., & Sathiaseelan, J. G. R. (2020). An exploratory of hybrid techniques on deep learning for image classification. *2020 4th international conference on computer, communication and signal processing (ICCCSP)* (pp. 1–4). IEEE. https://doi.org/10.1109/ICCCSP49186.2020.9315270

[30] Henry, T., Carré, A., Lerousseau, M., Estienne, T., Robert, C., Paragios, N., & Deutsch, E. (2020). Brain tumor segmentation with self-ensembled, deeply-supervised 3d u-net neural networks: A brats 2020 challenge solution. *International miccai brainlesion workshop* (pp. 327–339). Springer. https://doi.org/10.1007/978-3-030-72084-1_30

[31] Naseer, A., Yasir, T., Azhar, A., Shakeel, T., & Zafar, K. (2021). Computer-aided brain tumor diagnosis: Performance evaluation of deep learner CNN using augmented brain MRI. *International journal of biomedical imaging*, *2021*(1), 1-11. https://doi.org/10.1155/2021/5513500

[32] Kumar, A. (2023). Study and analysis of different segmentation methods for brain tumor MRI application. *Multimedia tools and applications*, *82*(5), 7117–7139. https://doi.org/10.1007/s11042-022-13636-y

[33] Srinivas, C., KS, N. P., Zakariah, M., Alothaibi, Y. A., Shaukat, K., Partibane, B., & Awal, H. (2022). Deep transfer learning approaches in performance analysis of brain tumor classification using MRI images. *Journal of healthcare engineering*, *2022*(1), 1-17. https://doi.org/10.1155/2022/3264367

[34] Agrawal, R., Sharma, M., & Singh, B. K. (2019). Segmentation of brain tumour based on clustering technique: Performance analysis. *Journal of intelligent systems*, *28*(2), 291–306. https://doi.org/10.1515/jisys-2017-0027

[35] Biratu, E. S., Schwenker, F., Ayano, Y. M., & Debelee, T. G. (2021). A survey of brain tumor segmentation and classification algorithms. *Journal of imaging*, *7*(9), 1–30. https://doi.org/10.3390/jimaging7090179